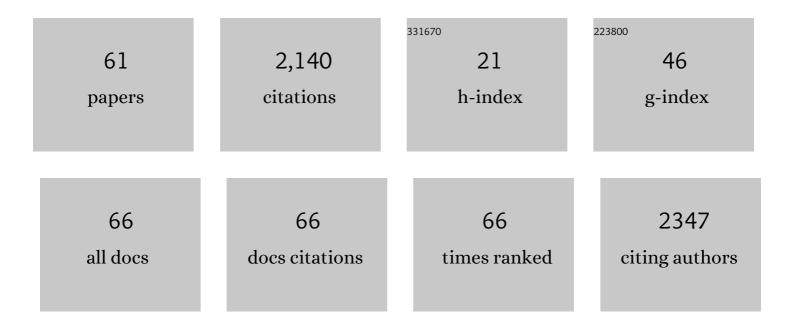
Kazuo Yamamoto

List of Publications by Year in descending order

Source: https://exaly.com/author-pdf/1269652/publications.pdf Version: 2024-02-01



#	Article	IF	CITATIONS
1	Denoising of series electron holograms using tensor decomposition. Microscopy (Oxford, England), 2021, 70, 255-264.	1.5	10
2	Denoising electron holograms using the wavelet hidden Markov model for phase retrieval—Applications to the phase-shifting method. AIP Advances, 2021, 11, .	1.3	8
3	Direct visualization of electric potential distribution in organic light emitting diode by phase-shifting electron holography. Applied Physics Express, 2021, 14, 075007.	2.4	1
4	Computational evaluation of sparse coding on off-axis electron holograms: comparison between charge-coupled device and direct-detection device cameras. Microscopy (Oxford, England), 2021, , .	1.5	3
5	Electron Holography Details the Tagish Lake Parent Body and Implies Early Planetary Dynamics of the Solar System. Astrophysical Journal Letters, 2021, 917, L5.	8.3	2
6	Phase-shifting electron holography for accurate measurement of potential distributions in organic and inorganic semiconductors. Microscopy (Oxford, England), 2021, 70, 24-38.	1.5	8
7	Lithium Transport Pathways Guided by Grain Architectures in Ni-Rich Layered Cathodes. ACS Nano, 2021, 15, 19806-19814.	14.6	23
8	Visualization of different carrier concentrations in n-type-GaN semiconductors by phase-shifting electron holography with multiple electron biprisms. Microscopy (Oxford, England), 2020, 69, 1-10.	1.5	4
9	Accurate Measurement of Electric Potential Distributions at the Interfaces in Solids Using Phase-shifting Electron Holography. Microscopy and Microanalysis, 2020, 26, 1956-1957.	0.4	0
10	Quantitative electric field mapping of a p–n junction by DPC STEM. Ultramicroscopy, 2020, 216, 113033.	1.9	15
11	Visualization of Lithium Transfer Resistance in Secondary Particle Cathodes of Bulk-Type Solid-State Batteries. ACS Energy Letters, 2020, 5, 2098-2105.	17.4	38
12	Simulation-Trained Sparse Coding for High-Precision Phase Imaging in Low-Dose Electron Holography. Microscopy and Microanalysis, 2020, 26, 429-438.	0.4	8
13	Dynamic imaging of lithium in solid-state batteries by operando electron energy-loss spectroscopy with sparse coding. Nature Communications, 2020, 11, 2824.	12.8	49
14	Direct visualization of the photovoltaic effect in a single-junction GaAs cell via <i>in situ</i> electron holography. Journal of Applied Physics, 2020, 128, .	2.5	0
15	Sparse coding and dictionary learning for electron hologram denoising. Ultramicroscopy, 2019, 206, 112818.	1.9	17
16	Direct Observation of a Liâ€lonic Spaceâ€Charge Layer Formed at an Electrode/Solidâ€Electrolyte Interface. Angewandte Chemie - International Edition, 2019, 58, 5292-5296.	13.8	43
17	Direct Observation of a Liâ€Ionic Spaceâ€Charge Layer Formed at an Electrode/Solidâ€Electrolyte Interface. Angewandte Chemie, 2019, 131, 5346-5350.	2.0	23
18	Accurate measurement of electric potentials in biased GaAs compound semiconductors by phase-shifting electron holography. Microscopy (Oxford, England), 2019, 68, 159-166.	1.5	12

ΚΑΖΟΟ ΥΑΜΑΜΟΤΟ

#	Article	IF	CITATIONS
19	Precise Potential Observation of a Biased GaAs p-n Junction by <i>in situ</i> Phase-shifting Electron Holography. Materia Japan, 2019, 58, 101-101.	0.1	0
20	High Precision Phase-Shifting Electron Holography with Multiple Biprisms for GaN Semiconductor Devices. Microscopy and Microanalysis, 2018, 24, 1554-1555.	0.4	3
21	Electric shielding films for biased TEM samples and their application to in situ electron holography. Microscopy (Oxford, England), 2018, 67, 178-186.	1.5	13
22	Quantitative <i>Operando</i> Visualization of Electrochemical Reactions and Li Ions in All-Solid-State Batteries by STEM-EELS with Hyperspectral Image Analyses. Nano Letters, 2018, 18, 5892-5898.	9.1	56
23	<i>Operando</i> observations of solid-state electrochemical reactions in Li-ion batteries by spatially resolved TEM EELS and electron holography. Microscopy (Oxford, England), 2017, 66, 50-61.	1.5	17
24	Rapid lowâ€ŧemperature synthesis of tetragonal singleâ€phase Li ₇ La ₃ Zr ₂ O ₁₂ . Journal of the American Ceramic Society, 2017, 100, 1313-1319.	3.8	13
25	Advanced electron holography techniques for in situ observation of solid-state lithium ion conductors. Ultramicroscopy, 2017, 173, 64-70.	1.9	9
26	Advanced electron holography techniques for in situ observation of solid-state lithium ion conductors. Ultramicroscopy, 2017, 176, 86-92.	1.9	1
27	In situ electron holography of electric potentials inside a solid-state electrolyte: Effect of electric-field leakage. Ultramicroscopy, 2017, 178, 20-26.	1.9	36
28	Precise measurement of electric potential, field, and charge density profiles across a biased GaAs p-n tunnel junction by in situ phase-shifting electron holography. Journal of Applied Physics, 2017, 122, 225702.	2.5	17
29	Crystallographic features related to a van der Waals coupling in the layered chalcogenide FePS3. Journal of Applied Physics, 2016, 120, .	2.5	41
30	Effects of sintering temperature on interfacial structure and interfacial resistance for all-solid-state rechargeable lithium batteries. Journal of Power Sources, 2016, 325, 584-590.	7.8	62
31	B23-O-12Visualization of potential map in a thin-film solar cell by high sensitivity phase-shifting electron holography. Microscopy (Oxford, England), 2015, 64, i58.2-i58.	1.5	0
32	Visualization of Electrochemical Reactions in All-Solid-State Li-Ion Batteries by Spatially Resolved Electron Energy-Loss Spectroscopy and Electron Holography. Materials Transactions, 2015, 56, 617-624.	1.2	11
33	B23-P-10Visualization of two-dimensional potential map in organic electroluminescent materials with phase-shifting electron holography. Microscopy (Oxford, England), 2015, 64, i116.2-i116.	1.5	1
34	Electrochemical reactions in an all-solid-state Li-ion battery observed by ex situ and in situ spatially-resolved TEM EELS. Microscopy and Microanalysis, 2015, 21, 1191-1192.	0.4	0
35	Analysis of GaAs Compound Semiconductors and the Semiconductor Laser Diode using Off-Axis Electron Holography, Lorentz Microscopy, Electron Diffraction Microscopy and Differential Phase Contrast STEM. Microscopy and Microanalysis, 2015, 21, 1975-1976.	0.4	0
36	B12-P-02Electron Holography Analysis with 3D Computer Simulation for Observing Potential Profile around Electrode/Solid-Electrolyte Interfaces. Microscopy (Oxford, England), 2015, 64, i86.1-i86.	1.5	0

Кагио Үамамото

#	Article	IF	CITATIONS
37	Dynamical observation of lithium insertion/extraction reaction during charge–discharge processes in Li-ion batteries by <i>in situ</i> spatially resolved electron energy-loss spectroscopy. Microscopy (Oxford, England), 2015, 64, 401-408.	1.5	9
38	Direct observation of dopant distribution in GaAs compound semiconductors using phase-shifting electron holography and Lorentz microscopy. Microscopy (Oxford, England), 2014, 63, 235-242.	1.5	26
39	Characterization of grain-boundary phases in Li7La3Zr2O12 solid electrolytes. Materials Characterization, 2014, 91, 101-106.	4.4	17
40	Preparation of thick-film LiNi1/3Co1/3Mn1/3O2 electrodes by aerosol deposition and its application to all-solid-state batteries. Journal of Power Sources, 2014, 272, 1086-1090.	7.8	49
41	In-situ Li7La3Zr2O12/LiCoO2 interface modification for advanced all-solid-state battery. Journal of Power Sources, 2014, 260, 292-298.	7.8	217
42	Nano-scale simultaneous observation of Li-concentration profile and Ti-, O electronic structure changes in an all-solid-state Li-ion battery by spatially-resolved electron energy-loss spectroscopy. Journal of Power Sources, 2014, 266, 414-421.	7.8	41
43	Electrically Conductive and Mechanically Elastic Titanium Nitride Ceramic Microsprings. Journal of Nanoscience and Nanotechnology, 2014, 14, 4292-4296.	0.9	1
44	Vortex magnetic structure in framboidal magnetite reveals existence of water droplets in an ancient asteroid. Nature Communications, 2013, 4, 2649.	12.8	30
45	Electrochemical properties of an all-solid-state lithium-ion battery with an in-situ formed electrode material grown from a lithium conductive glass ceramics sheet. Journal of Power Sources, 2013, 241, 583-588.	7.8	47
46	Development of advanced electron holographic techniques and application to industrial materials and devices. Microscopy (Oxford, England), 2013, 62, S29-S41.	1.5	14
47	Direct observation of lithium-ion movement around an in-situ-formed-negative-electrode/solid-state-electrolyte interface during initial charge–discharge reaction. Electrochemistry Communications, 2012, 20, 113-116.	4.7	68
48	High lithium ion conductive Li7La3Zr2O12 by inclusion of both Al and Si. Electrochemistry Communications, 2011, 13, 509-512.	4.7	236
49	Characterization of the interface between LiCoO2 and Li7La3Zr2O12 in an all-solid-state rechargeable lithium battery. Journal of Power Sources, 2011, 196, 764-767.	7.8	326
50	Dipolar ferromagnetic phase transition in Fe3O4 nanoparticle arrays observed by Lorentz microscopy and electron holography. Applied Physics Letters, 2011, 98, .	3.3	55
51	Dynamic Visualization of the Electric Potential in an Allâ€Solidâ€State Rechargeable Lithium Battery. Angewandte Chemie - International Edition, 2010, 49, 4414-4417.	13.8	242
52	Phase-shifting electron holography for atomic image reconstruction. Journal of Electron Microscopy, 2010, 59, S81-S88.	0.9	7
53	Direct visualization of dipolar ferromagnetic domain structures in Co nanoparticle monolayers by electron holography. Applied Physics Letters, 2008, 93, 082502.	3.3	55
54	Electron holography of single-crystal iron nanorods encapsulated in carbon nanotubes. Journal of Applied Physics, 2007, 101, 014323.	2.5	21

Казио Үамамото

#	Article	IF	CITATIONS
55	Electron holographic observation of micro-magnetic fields current-generated from single carbon coil. Ultramicroscopy, 2006, 106, 314-319.	1.9	30
56	Reconstruction technique for off-axis electron holography using coarse fringes. Ultramicroscopy, 2006, 106, 486-491.	1.9	16
57	Off-axis electron holography without Fresnel fringes. Ultramicroscopy, 2004, 101, 265-269.	1.9	24
58	Evaluation of high-precision phase-shifting electron holography by using hologram simulation. Surface and Interface Analysis, 2003, 35, 60-65.	1.8	14
59	Hologram simulation for off-axis electron holography. Ultramicroscopy, 2000, 85, 35-49.	1.9	19
60	Lorentz Microscopy of Magnetic Granular Films. Physical Review Letters, 1999, 83, 1038-1041.	7.8	12
61	Visualization of depletion layer in AlGaN homojunction p–n junction. Applied Physics Express, 0, , .	2.4	3